Direct Simulation of Shock Layer Plasmas

E. D. Farbar and I. D. Boyd

Dept. of Aerospace Engineering, University of Michigan, 1320 Beal Ave., Ann Arbor MI, 48109

Abstract.
Approximate models of the electric field used with the DSMC method all impose quasi-neutrality everywhere in the shock layer plasma. The shortcomings of these models are examined in this study by simulating a weak shock layer plasma with a coupled DSMC-Particle-In-Cell (PIC) method. The stagnation streamline of an axisymmetric shock layer is simulated for entry velocities in air that correspond to both lunar and Mars return trajectories. The atmospheric densities, particle diameters and chemical reaction rates are varied from the actual values to make the computations tractable while retaining the mean free path of air at 85km altitude. In contrast to DSMC flow field predictions, regions of non-neutrality are predicted by the DSMC-PIC method, and the electrons are predicted to be isothermal. Perhaps the most important result of this study is that the DSMC-PIC results at both reentry energies yield a 14% increase in heat flux to the vehicle surface relative to the DSMC results. Rather unintuitively, this is mostly due to an increase in ion flux to the surface, rather than the potential energy gained by each ion as it traverses the plasma sheath. In this study, an approximate electric field model is presented, with the goal of accounting for this heat flux augmentation without the need for a computationally expensive DSMC-PIC calculation of the entire flow-field. Convective heat flux results obtained with new electric field model are compared to results from the rigorous DSMC-PIC calculations.

INTRODUCTION

During the reentry of a vehicle into the atmosphere at super-orbital velocities, a weakly ionized plasma is formed in the shock layer. This plasma affects the structure of the flow field, the heat transfer to the vehicle surface and the ability to maintain communication with the vehicle. The flight environment during reentry is difficult to reproduce experimentally, so robust and accurate numerical models of the fluid and plasma physics are necessary for mission design.

A notional schematic of a hypersonic shock layer and the associated plasma is given in Figure 1. In the bulk plasma region of the shock layer, the gas is quasi-neutral due to the presence of an ambipolar electric field. However, in the free diffusion region upstream of the bow shock and in the sheath near the vehicle surface, charge separation occurs.

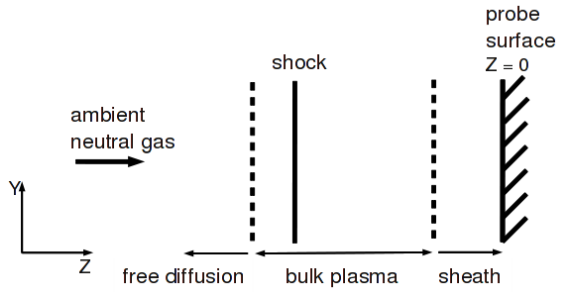

FIGURE 1. Location of the plasma generated in a hypersonic shock layer.

When computing ionized gas flows, the standard DSMC modeling approach is to use an approximate plasma model[1, 2, 3, 4] derived from the ambipolar diffusion assumption to simulate the shock layer plasma in it's entirety. While this approach is attractive from a simplicity standpoint, the limitations of this approach have not been assessed. The shortcomings of these approximate plasma models are examined in this study by simulating a shock layer plasma with a coupled DSMC[5]- PIC[6] technique. Additionally, a new approximate electric field model is suggested to address some of the shortcomings of the aforementioned models.

SIMPLIFIED SHOCK LAYER MODEL

The stagnation streamline of an axisymmetric shock layer is simulated for entry velocities in air of 11.37 km/s and 13km/s using the method developed by Bird for simulation of an axisymmetric blunt body flow [5]. A reentry velocity of 11.37 km/s is chosen because the Apollo-era experimental FIRE II vehicle entered at this velocity, and a typical Mars return velocity would be approximately 13 km/s. The neutral gas is composed of N, O, N_2, O_2 and NO particles, and the plasma is composed of N^+, O^+, N_2^+, O_2^+ and NO^+ ions as well as electrons. The free stream density for the two cases presented in this work is $2\times10^{14}m^{-3}$, much lower than the density experienced by the FIRE II vehicle at the strongly rarefied, 85 km trajectory point. To model the atmospheric mean free path at an altitude of 85 km in the simplified shock layer model, the particle diameters used in the VHS molecular model are increased by a factor of $\sqrt{1\times10^6}$ from the values for air given in Ref. [7]. Additionally, to retain the degree of ionization experienced by the FIRE II vehicle at the 85 km trajectory point[7], the chemical rate coefficients are increased by a factor of 5×10^5 from the baseline values given in Ref. [7]. This simplified modeling approach is similar to that taken by Kawamura et al. to simulate a plasma reactor using the PIC-Monte-Carlo-Collision (MCC) method[8]. The vehicle surface is assumed to be fully catalytic to the recombination of ions and electrons, and not catalytic to the recombination of neutral particles. Particles that strike the surface accommodate fully to the surface temperature of 460 K, and are reflected diffusely.

NUMERICAL TECHNIQUE

The DSMC module uses a code called MONACO[9], developed specifically for hypersonic flow simulations. Models are implemented in the code for rotational[10] and vibrational energy exchange[11], and chemical reactions in this study are simulated using the Total Collision Energy model[12]. When not coupled to the PIC module, the DSMC collision routine is sub-cycled to account for the high collision rate of the electrons with other particles, and the ambipolar diffusion model of Boyd[4] is used to maintain approximate charge neutrality. The electric field is not explicitly calculated. The simulation time step is limited by the collision time of the heavy particles.

The PIC module solves the electrostatic Poisson equation using the charge density at each grid node, calculated using the Charge-In-Cloud (CIC)[6] interpolation technique at each simulation time step. The electric field computed at each grid node is interpolated back to the individual particle locations using the same CIC technique. A zero electric field boundary condition is specified at the free stream, and the potential of the surface of the vehicle is fixed at 0 V. The electric field at particle locations is assumed to be constant over a simulation time step, and when the simulation is run in coupled DSMC-PIC mode, the charged particles are accelerated using this field. The DSMC-PIC simulation time step is limited by the cell transit time of the electrons.

The same computational grid is used for the DSMC and PIC algorithms in this study. The grid is refined to approximately one-fifth the electron Debye length everywhere in the domain, and this is always smaller than the mean free path. The weight factor of the simulator particles is selected to yield approximately 10 charged particles per cell in the peak plasma density region, and approximately 300 000 particles are simulated overall. The simulation is converged when the number of simulator particles in the domain, the total energy in the domain and the current to the vehicle surface (only in the coupled DSMC-PIC calculations) reach a steady state. The simulation time for the coupled DSMC-PIC computations presented here is approximately 240 CPU hours.

SELF-CONSISTENT SIMULATION RESULTS

The results from the coupled DSMC-PIC simulations of both the U_∞=11.37 km/s and U_∞=13 km/s cases are presented in this section. Figure 2(a) shows the potential and electric fields predicted along the stagnation streamline for both cases. The potential drop in the sheath is slightly larger in the higher velocity case due to the higher temperature of the electrons in this case. Other than that, the trends observed in the flow field predictions are very similar in both cases and only those of the 11.37 km/s case will be discussed further in this section.

Figure 2(b) shows the translational, rotational, vibrational and electron translational temperatures along the stagnation streamline. The flow is in a strong degree of thermal nonequilibrium. While the DSMC results predict thermal equilibrium between the electron and vibrational temperatures, the DSMC-PIC results predict nearly isothermal electrons. This is owing to the fact that electrons are now essentially reflected from the sheath region, and are able to move upstream of the shock unrestrained by the ions. Physically, both of these effects serve to broaden the electron energy

distribution in the respective regions of the flow.

Figure2(c) shows the predicted ion and electron number density along the stagnation streamline. Also shown on this figure is the magnitude of the predicted charge separation. In the bulk plasma, the charged species diffuse at approximately the same rate, and the flow is approximately charge neutral. Thus, the DSMC and DSMC-PIC results are nearly identical in this region. However, near the surface in the sheath region, the electron density falls off rapidly as the electrons are turned back by the strong potential gradient in the sheath. The ions are accelerated by the same gradient and their density falls off slightly, but it increases very near the surface due to the collisionality of the sheath in this simple shock layer model. Neither of these effects can be predicted by the DSMC model utilizing the ambipolar diffusion assumption. In the region upstream of the shock where the bulk plasma interacts with the ambient neutral gas, the concentration of charged particles becomes too low to support the electric field necessary to maintain charge neutrality. Thus, the DSMC-PIC results predict a negative charge separation in this region, while the DSMC results of course maintain charge neutrality there.

The DSMC-PIC results for the 11.37 km/s case predict a 14% increase in the convective heat flux at the stagnation point relative to the DSMC results, while those for the 13 km/s case predict a 13% increase in convective heat flux. Figure 3(a) shows a breakdown of heat flux components by species for the 11.37 km/s case, along with the total heat flux to the vehicle surface, from both the DSMC and DSMC-PIC simulations. The error bars on this figure represent the 1σ error on the heat flux measurement, and are produced during the respective simulations. Increases in heating are due to both the primary acceleration of the ions, and the secondary acceleration of neutral particles upon collisions with energetic ions. The acceleration of ions in the sheath region has a focusing effect, allowing ions to reach the surface that would have normally traveled away from the stagnation region. Thus, the increase in ion flux to the surface predicted by the DSMC-PIC method, as demonstrated in Figure 3(b), plays a prominent role in the overall heat flux increase seen in the DSMC-PIC results.

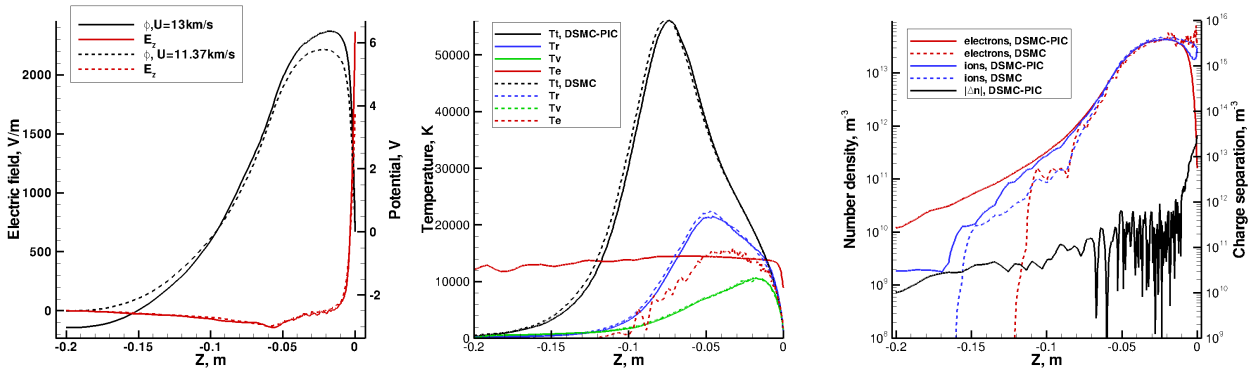

(a) Electric and potential fields for both the U_∞=11.37 km/s and U_∞=13 km/s cases.

(b) Mode temperatures for 11.37 km/s case.

(c) Charged species number density for 11.37 km/s case.

FIGURE 2. Flow field properties computed using the DSMC-PIC technique. Comparison to DSMC results where applicable.

APPROXIMATE ELECTRIC FIELD MODEL

With current computing resources, it is not possible to apply the DSMC-PIC technique to the simulation of actual Earth reentry flight conditions due to its large computational expense. Thus, a new approximate electric field model has been formulated for use with the DSMC method. This model combines some of the components of previous DSMC plasma models. The goal is to reproduce the heat flux increase seen in the DSMC-PIC results, without significantly increasing the computational resources required for a DSMC calculation.

The model has two discrete components. In the bulk plasma region, where the DSMC-PIC results indicate that the plasma is quasi-neutral, a solution of the Boltzmann relation is used to obtain the plasma potential. The Boltzmann relation is given in Equation 1, where e is the elementary charge, k the Boltzmann constant, T_e the electron translational temperature, n_i is the ion number density and n_i, o is a reference density. The ion number density is used in Equation 1 in place of the electron number density, owing to the fact that the plasma is quasi-neutral in the bulk region.

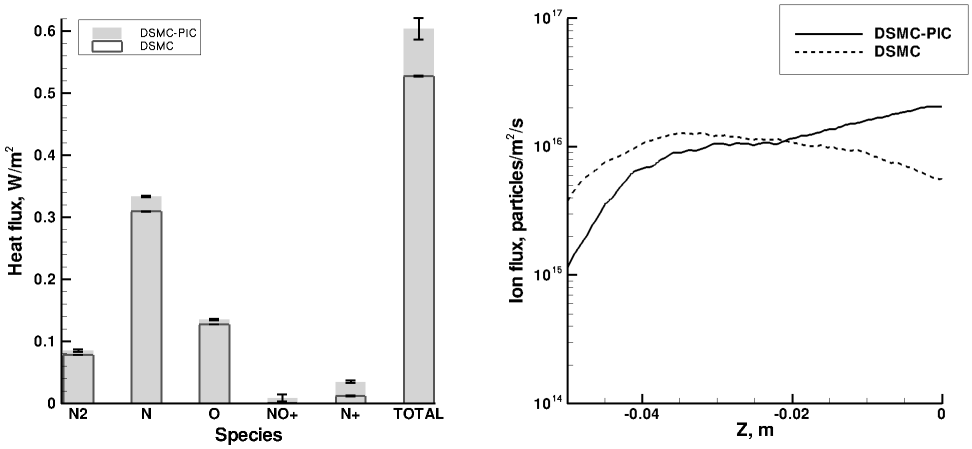

(a) Surface heat flux components.

(b) Ion flux in the near wall region.

FIGURE 3. Results from the 11.37 km/s case.

$$n_i = n_{i,o} exp\left(\frac{e\phi(z)_{bulk}}{kT_e}\right) \tag{1}$$

The Boltzmann relation is coupled to a quadratic expression for the potential drop in the plasma sheath given by Equation 2. In that equation, T_i is the ion translational temperature, m_e and m_i are the electron and ion masses, z_s is the sheath width given by Equation 3 with the Debye length λ_D also defined, and $\Delta\phi_w$ is the potential drop at the vehicle surface given by Equation 5. The form of Equation 2 implies the assumption of one-dimensional, collisionless plasma dynamics in the sheath. Both Equations 1 and 2 require the assumption that the electrons can be described by a Maxwellian velocity distribution in the bulk plasma region[13].

$$\phi(z)_{sheath} = -\frac{\Delta\phi_w}{z_s^2}z^2 + \frac{2\Delta\phi_w}{z_s}z + (\phi(z_s)_{bulk} - \Delta\phi_w) \tag{2}$$

$$z_s = C\lambda_D \tag{3}$$

$$\lambda_D = \sqrt{\frac{\varepsilon_o kT_e}{n_e e^2}} \tag{4}$$

$$\Delta\phi_w = \frac{kT_e}{e} ln\left[\frac{T_e}{T_i}\frac{m_i}{m_e}\right] \tag{5}$$

In the new electric field model, the electrons are constrained to move throughout the grid with the average ion velocity, and only the ions are accelerated by the computed electric field. The model is called the Boltzmann Quadratic Sheath (BQS) Model. The physical limitations of the model are that it cannot accurately predict i) the region of charge separation upstream of the shock layer seen in Figure 2(c), ii) the electron temperature in the sheath region, and iii) the electron density in the sheath region. However, it contains the physics necessary to model the important heat flux augmentation predicted by the DSMC-PIC results. The BQS model is implemented by obtaining the values T_e, T_i and n_e from the bulk plasma region of a DSMC flow field solution for use in computing the constants $\Delta\phi_w$ and λ_D in Equation 2. The average ion mass is set to the mass of atomic nitrogen ions in this work, as they are the predominant ionic species in the sheath region. There is ambiguity in the choice of the multiplier C for the sheath width z_s, as the definition of a sheath width is fundamentally arbitrary. For the calculations presented in this work, the value of the multiplier is obtained from the location at which charge separation first occurs in the DSMC-PIC results, and the sheath width in both cases is approximately $z_s = 8\lambda_D$. In practice, this value could be varied to obtain the 'worst-case' estimate of heat flux augmentation.

Results

The BQS model is applied to both the 11.37 km/s and 13km/s shock layer cases with encouraging results. Figures 4(a) and 4(b) show the ion number densities predicted using the BQS model, those given by the DSMC-PIC results, and those given by the DSMC results for both cases. The BQS model captures the trends of the ion density profiles from the DSMC-PIC results well. Figures 5(a) and 5(b) show the ion flux near the surface predicted by the BQS model, and the DSMC and DSMC-PIC results for both cases. Again, the BQS model captures the character of the ion flux better than the ambipolar diffusion model did, however it does under-predict the net ion flux reaching the surface. Figure 6(a) shows a comparison of the electric and potential fields given by the BQS model to those predicted by the DSMC-PIC technique for the 11.37 km/s case. The agreement is generally quite good, although very near the wall, the quadratic form of the potential used in the BQS model does under-predict the electric field. Lastly, Figure 6(b) shows the heat flux prediction using the BQS model, as well as the DSMC and DSMC-PIC techniques, for the 11.37 km/s case. Although the BQS model does not capture all of the heat flux increase predicted by the DSMC-PIC results, it does predict an increase of 12% relative to the DSMC results, which for this case is within the error associated with the statistical uncertainty of the DSMC-PIC simulation. The heat flux results for the Mars return case at 13 km/s, not shown here, are not quite as encouraging. The BQS model in combination with the DSMC method only predicts an 8% increase in the convective heat flux, lower than the 13% increase predicted by the rigorous DSMC-PIC technique.

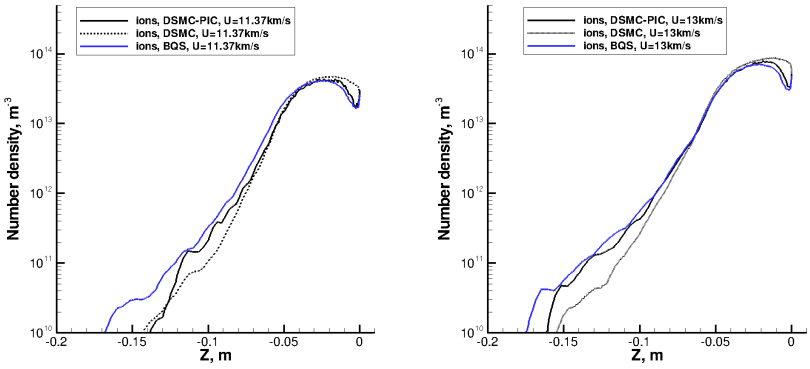

(a) 11.37 km/s case. *(b)* 13 km/s case.

FIGURE 4. Ion number density along the stagnation streamline predicted using the BQS model.

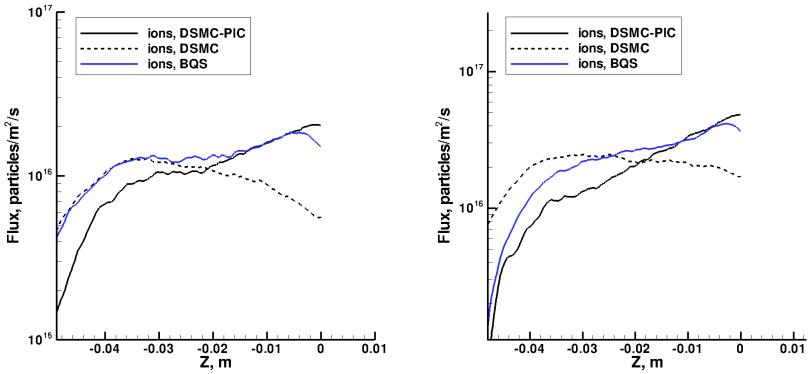

(a) 11.37 km/s case. *(b)* 13 km/s case.

FIGURE 5. Ion flux along the stagnation streamline predicted using the BQS model.

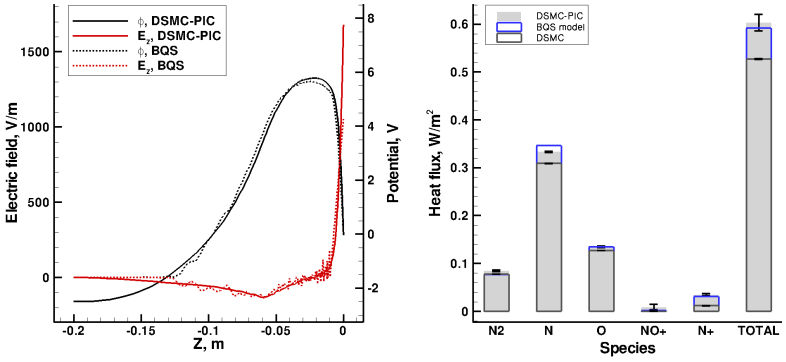

(a) Electric and potential fields. *(b)* Surface heat flux components.

FIGURE 6. Results for the 11.37 km/s case predicted using the BQS model.

CONCLUSIONS

A rigorous DSMC-PIC technique was used to simulate a weakly ionized plasma in a simplified shock layer representative of that formed during entry of a hypersonic vehicle into the Earth's atmosphere. This self-consistent simulation of the plasma represents the first assessment of the accuracy of the standard DSMC plasma modeling approach based on the ambipolar diffusion approximation. Compared to the DSMC results, the DSMC-PIC technique predicts differences in the electron translational temperature, the number densities of charged species in the sheath region and downstream of the shock location, and an increase in the heat flux to the vehicle surface. For an Earth entry mission where the vehicle spends a large amount of time in the rarefied region of the atmosphere, the predicted increase in the overall heat flux may affect the vehicle heat shield design. A new approximate electric field model developed to capture the heat flux augmentation has been implemented with encouraging results. It has the ability to reproduce the DSMC-PIC heat flux results, and can be applied to computations at actual Earth entry conditions.

ACKNOWLEDGMENTS

The authors gratefully acknowledge the financial support provided by NASA grant NCC3-989.

REFERENCES

1. G. A. Bird, "Direct Simulation of Typical AOTV Entry Flows," in *38th AIAA Aerospace Sciences Meeting and Exhibit*, AIAA Paper 86-1310, June 1986.
2. J. C. Taylor, A. B. Carlson, and H. A. Hassan, *Journal of Thermophysics and Heat Transfer* **8**, 478–485 (1994).
3. M. A. Gallis, and J. K. Harvey, "Ionization Reactions and Electric Fields in Plane Hypersonic Shock Waves," in *Rarefied Gas Dynamics*, AIAA, New York, 1992, vol. 160 of *Progress in Astronautics and Aeronautics*, pp. 234–244.
4. I. D. Boyd, *Physics of Fluids* **9**, 4575–4584 (1997).
5. G. A. Bird, *Molecular Gas Dynamics and the Direct Simulation of Gas Flows*, Oxford Science Publications, 1994.
6. R. W. Hockney, and J. W. Eastwood, *Computer Simulation Using Particles*, McGraw-Hill Inc., 1981.
7. E. D. Farbar, and I. D. Boyd, "Simulation of FIRE II Reentry Flow Using the Direct Simulation Monte Carlo Method," in *40th AIAA Thermophysics Conference, Seattle, WA*, AIAA Paper 2008-4103, June 2008.
8. E. Kawamura, A. J. Lichtenberg, M. A. Lieberman, and J. P. Verboncoeur, *Physics of Plasmas* **16**, 122114 (2009).
9. S. Dietrich, and I. D. Boyd, *Journal of Computational Physics* **126**, 328–342 (1996).
10. I. D. Boyd, *Physics of Fluids* **2**, 447–452 (1989).
11. I. D. Boyd, *Physics of Fluids* **3**, 1785–1791 (1991).
12. G. A. Bird, "Monte Carlo Simulation in an Engineering Context," in *Rarefied Gas Dynamics*, edited by S. S. Fisher, AIAA, New York, 1981, vol. 74 of *Progress in Astronautics and Aeronautics*, pp. 239–255.
13. M. A. Lieberman, and A. J. Litchenberg, *Principles of Plasma Discharges and Materials Processing*, Wiley-Interscience, 2005.